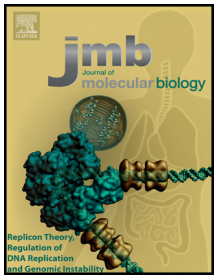

Exploring the Minimally Frustrated Energy Landscape of Unfolded ACBP

Valéry Ozenne[1,†], Jeffrey K. Noel[2,†], Pétur O. Heidarsson[3], Søren Brander[3], Flemming M. Poulsen[3], Malene Ringkjøbing Jensen[1], Birthe B. Kragelund[3], Martin Blackledge[1] and Jens Danielsson[3,4]

*1 - **Protein Dynamics and Flexibility,** Institut de Biologie Structurale Jean-Pierre Ebel, CNRS-CEA-UJF UMR 5075, 6, 38000, France*
*2 - **Center for Theoretical Biological Physics,** Rice University, Houston, TX 77005-1827, USA*
*3 - **Structural Biology and NMR Laboratory,** Department of Biology, University of Copenhagen, Ole Maaløes Vej 5, DK-2200 Copenhagen, Denmark*
*4 - **Department of Biochemistry and Biophysics,** Arrhenius Laboratories of Natural Sciences, Stockholm University, SE-106 91 Stockholm, Sweden*

Correspondence to Jens Danielsson
http://dx.doi.org/10.1016/j.jmb.2013.10.031
Edited by C. Kalodimos

Abstract

The unfolded state of globular proteins is not well described by a simple statistical coil due to residual structural features, such as secondary structure or transiently formed long-range contacts. The principle of minimal frustration predicts that the unfolded ensemble is biased toward productive regions in the conformational space determined by the native structure. Transient long-range contacts, both native-like and non-native-like, have previously been shown to be present in the unfolded state of the four-helix-bundle protein acyl co-enzyme binding protein (ACBP) as seen from both perturbations in nuclear magnetic resonance (NMR) chemical shifts and structural ensembles generated from NMR paramagnetic relaxation data. To study the nature of the contacts in detail, we used paramagnetic NMR relaxation enhancements, in combination with single-point mutations, to obtain distance constraints for the acid-unfolded ensemble of ACBP. We show that, even in the acid-unfolded state, long-range contacts are specific in nature and single-point mutations affect the free-energy landscape of the unfolded protein. Using this approach, we were able to map out concerted, interconnected, and productive long-range contacts. The correlation between the native-state stability and compactness of the denatured state provides further evidence for native-like contact formation in the denatured state. Overall, these results imply that, even in the earliest stages of folding, ACBP dynamics are governed by native-like contacts on a minimally frustrated energy landscape.

Introduction

The unfolded state of a protein is an essential reference point for understanding the molecular processes in which the protein is involved, such as folding leading to function, folding upon binding of intrinsically disordered proteins, misfolding, and aggregation [1–3]. The unfolded polypeptide chain is not merely a randomly sampled statistical coil but, rather, possesses secondary structure propensity (SSP) and transient long-range contacts. These structural biases can potentially affect the productive on-pathway events in protein folding [4–7].

Studies of unfolded states are complicated by the fact that, under native conditions, the fraction of unfolded protein is typically very low. The unfolded population can be increased by mutagenesis, deletions [8], or more often using chaotropic chemicals or acid to shift the protein equilibrium toward an unfolded state [9].

Acyl co-enzyme binding protein (ACBP) is a small (86 residues) four-helix-bundle, fast-folding protein (Fig. 1) [10]. The unfolded ensemble of ACBP has

Please cite this article as: Ozenne Valéry, et al, Exploring the Minimally Frustrated Energy Landscape of Unfolded ACBP, J Mol Biol (2013), http://dx.doi.org/10.1016/j.jmb.2013.10.031

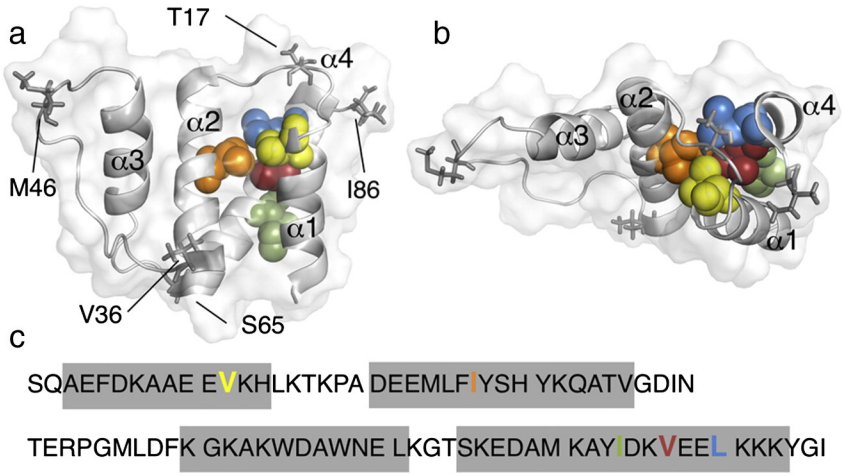

Fig. 1. (a and b) Side and top view of acyl co-enzyme A binding protein (ACBP) (PDB ID: 1NTI). Parts of the hydrophobic core are shown in colored sphere representation and focus on V12 (yellow), I27 (orange), I74 (green), V77 (red), and L80 (blue). The positions of the cysteine insertions are shown as sticks. The primary structure is shown in (c) using the same color coding as in (a) and (b). The positions of helices α1–α4 are shown as boxes on the primary structure.

been extensively studied through both acidic and chaotropic denaturation. The unfolded ensemble has been shown to retain a significant amount of residual structure even in the presence of high concentrations of denaturant [11,12]. At low pH, all four helical segments show secondary chemical shifts corresponding to formation of transient residual helical structure, most prominent in helices α2 and α4 [7,13]. Nuclear magnetic resonance (NMR) paramagnetic relaxation enhancement (PRE) [11,12,14], chemical shift analysis [15], residual dipolar couplings [16], and more recently fluorescence resonance energy transfer (FRET) [17] and molecular dynamics [18] have revealed the presence of long-range contacts in the denatured state of ACBP. These long-range contacts are linked to the presence of residual secondary structure [15]. This indicates that either transient helical structure increases the population of long-range contacts or the presence of long-range contacts cooperatively induces helix formation. These long-range contacts in the acid-unfolded state of ACBP have been shown, both experimentally and *in silico*, to involve contacts among helices α2, α3, and α4 [14,15,17].

Although the determinants of SSPs are quite well known, such that SSP can be predicted from primary structure with reasonable accuracy [19], the determinants of the long-range contacts in the unfolded ensemble are less well understood. Hydrophobic interactions are expected to be of importance for the formation of initial productive long-range contacts [1], while electrostatic interactions seem less prominent in this early stage of protein folding [20]. Nevertheless, the development of a complete understanding of the hierarchy of transient long-range interactions in unfolded proteins remains a key challenge.

The apparent paradoxes in protein folding are generally explained by the minimal frustration theory [21] and by the introduction of a funnel-shaped free-energy landscape [22]. Folding and structure are tightly linked, with evolutionary selection and conservation of primary structure encoding secondary and tertiary structures in the native state, all structural levels being operative already in the unfolded state as secondary structure propensity and on-pathway long-range interactions. In addition, long-range contacts, native and non-native, formed in the unfolded state may serve as gatekeepers to protect from misfolding and aggregation [23].

In this study, we focus on understanding the determinants of long-range contacts in the unfolded state ensemble and how perturbations of these modulate the free-energy landscape. We use NMR PRE measurements for acid-unfolded ACBP along with the recently developed statistical ensemble selection tool ASTEROIDS [24] to calculate representative ensembles of structures that fulfill the experimental data. Single-point mutations of conserved hydrophobic residues known to be involved in formation of the transition state, that is, residues with relatively high φ-values [25], are used to systematically perturb native-like long-range contacts and thereby characterize how these contacts shape the unfolded ensemble. We find that replacement of a single bulky hydrophobic side chain significantly affects the unfolded ensemble and that the most prominent effects are seen when perturbing those contacts formed earliest along the *in silico* folding pathway of ACBP.

Please cite this article as: Ozenne Valéry, et al, Exploring the Minimally Frustrated Energy Landscape of Unfolded ACBP, J Mol Biol (2013), http://dx.doi.org/10.1016/j.jmb.2013.10.031

Results

The acid-unfolded ACBP exhibits both non-native and native long-range contacts

In order to obtain an almost fully unfolded ACBP, we used low protein concentration and acid denaturation (pH 2.3) that has previously been shown to induce an unfolded monomeric population that is larger than 99.9% [13] (Supplementary Fig. 1). One advantage of using acid as denaturant is to reduce the complexity of the solution compared to guanidinium chloride (GdmCl) or urea. To obtain information about long-range contacts in the unfolded ensemble, we attached nitroxide spin labels to the protein at different positions. Following the protocol described in Ref. [14], we constructed four single cysteine variants of ACBP: T17C, V36C, M46C and I86C, all of which are located in loop or turn regions in the native state (Fig. 1). The spin label MTSL was covalently bound to each of the cysteines by disulfide linkage, and PREs were measured for each cysteine variant. The program Flexible-meccano [26,27] was used to generate a large pool (50,000) of statistical coil conformers of ACBP, and the ensemble selection algorithm ASTEROIDS [24] was used to select five different ensembles, each consisting of 200 structures, that were representative of the experimental PREs [24,28].

The distance distribution in the selected ASTEROIDS ensembles was compared to that of the statistical coil ensemble (the Flexible-meccano pool) via a generalized contact map using the metric $\Delta_{ij} = \log_{10}(\langle d_{ij}\rangle/\langle d_{ij}^0\rangle)$ where $\langle d_{ij}\rangle$ is the average distance between residues i and j in the ASTEROIDS ensemble and $\langle d_{ij}^0\rangle$ is the average distance in the coil model. For wild-type ACBP, at pH 2.3, the contact map displays the presence of both native-like and non-native-like contacts (Fig. 2). The long-range contacts mainly involve regions corresponding to helix α2 in contact with those of α3 and α4 and contacts between regions corresponding to helices α1 and α4. This is in agreement with contacts previously identified using restrained molecular dynamics simulations [12]. The regions corresponding to helices α1–α4 in the native state will be hereafter referred to as α1–α4, if not stated otherwise. This nomenclature is unrelated to whether these regions are forming secondary structure in the denatured ensemble. We found short ensemble distances between α2 and α4 that may reflect native-like contacts, although the overall strongest contacts are the non-native contacts between the C-terminal region of α4 and the C-terminal region of α2 and loop II (Figs. 1 and 2). Furthermore, native-like helix–helix contacts were also found between regions α1 and α4, from now on denoted α1α4, and α2α3, but these contacts are less prominent than the α2-to-α4 contact. This shows that the α2α4 contact is more populated and may be formed early along the folding pathway, while the less prominent contacts are formed later on, putatively as a subsequent conditional event. Several native-like long-range contacts were not detected in the denatured state, for example, the α1α2 contact has no preference for formation in the unfolded state. This is in agreement with findings from a peptide study that helix α2 alone

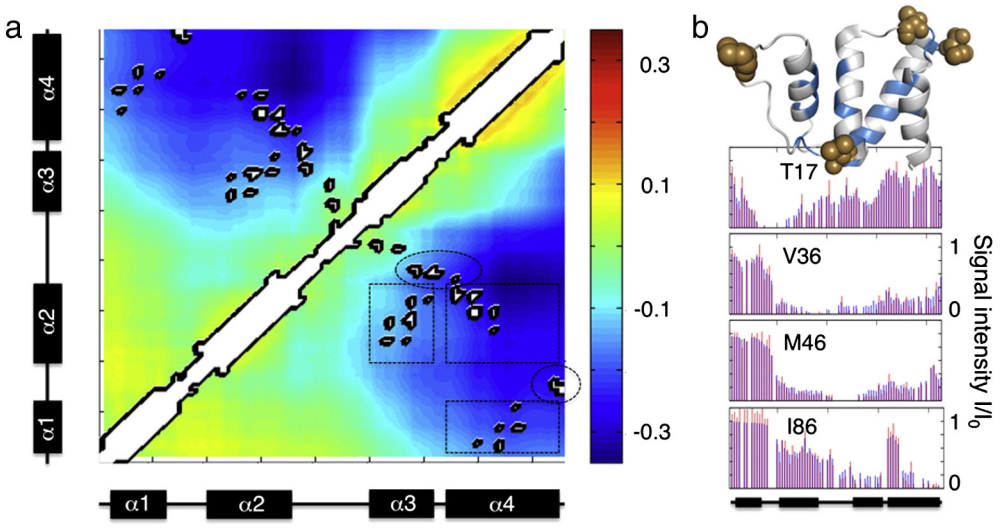

Fig. 2. In (a), a generalized contact map of an ensemble of acid-unfolded ACBP is shown, the colors represent $\Delta_{ij} = \log(\langle d_{ij}\rangle/\langle d_{ij}^0\rangle)$ showing a general more collapsed state than the statistical coil. Close native-state contacts are shown in white with black contours. The secondary structure elements, α1–α4, are schematically shown as bars. In (b), the spin-labeling positions are mapped onto the structure and measured, and ensemble-derived PREs are shown as red and blue bars, respectively.

Please cite this article as: Ozenne Valéry, et al, Exploring the Minimally Frustrated Energy Landscape of Unfolded ACBP, J Mol Biol (2013), http://dx.doi.org/10.1016/j.jmb.2013.10.031

needs a carrier scaffold to keep it in solution while anchoring the soluble α1 is entropically disfavored [29].

From the selected ASTEROIDS ensembles, the statistical coil ensemble, and the known distances in the natively folded protein, a generalized free-energy difference ΔG_C for native-like contact formation (Fig. 2) may be estimated as

$$\Delta G_C = -2.3RT \log K_C \quad (1)$$

where the equilibrium constant for formed contacts $K_C = p_C/(1 - p_C)$ can be calculated using the contact population p_C, defined as:

$$p_c = \left\langle \frac{\langle d_C^{obs} \rangle - \langle d_C^{coil} \rangle}{d_C^{fold} - \langle d_C^{coil} \rangle} \right\rangle_{ij} \quad (2)$$

where $\langle d_C^{obs} \rangle$ is the ASTEROIDS ensemble interhelical distance, $\langle d_C^{coil} \rangle$ is the corresponding distance in the coil model, d_C^{fold} is the distance in the natively folded state, and $\langle\rangle_{ij}$ denotes the average over all contact pairs *ij* in the contact regions. The estimated ΔG_C values at $T = 298$ K for both native-like contact between helical regions and specific long-range contacts are listed in Table 1. The lowest free-energy cost and, thus, the most probable contact is found for α2α4 contacts with $\Delta G_C = 0.5$ kcal/mol, while the least likely of the narrow native-state long-range contacts in the unfolded state is α2α3 with $\Delta G_C = 1.0$ kcal/mol corresponding to a contact population of 0.16.

In addition to comparing the experimentally determined PREs with those back-calculated from the ASTEROIDS ensembles, the selected ensemble can also be validated by comparing experimentally determined hydrodynamic radii, R_H, with the radii of gyration, R_G, of the ASTEROIDS ensemble (Supplementary Fig. 2). R_H and R_G scale similarly with the degree of disorder and give a crude estimate of the validity of the selected ensembles. In our PFG-NMR diffusion experiments, we obtained $R_H = 25.2 \pm 0.2$ Å for acid-unfolded wild-type ACBP, in agreement with earlier findings [12] (Supplementary Fig. 3). The corresponding ASTERIODS-derived radius of gyration is 23.6 ± 4 Å from which R_H can be estimated to be 25.4 ± 2 Å, using the empirical relationship $R_H^{-1} = (0.0212 + 0.428\ R_G^{-1})^{-1}$ [12], in good agreement with the experimental data. Similarly, the predicted R_H of the statistical coil model ensemble generated by Flexible-meccano is 27 ± 6 Å compared to the expected 28 Å for completely denatured ACBP [30].

Molecular dynamical simulations support the selected ensembles

The contact map of unfolded wild-type ACBP shows a bias toward a more compact state with several native-like long-range contacts populated already in the strongly denatured state. The important question is whether these contacts are productive, that is, are they formed along the folding pathway and/or do they initiate cooperative folding? As these structural states are transient and very short-lived, direct experimental observation is difficult. In order to obtain more detailed information on the importance of these early transient contacts, we performed folding simulations of ACBP, using a standard, coarse-grained, native-centric protein model.

The simulations qualitatively reproduced the major features of the folding pathway of ACBP characterized experimentally, which we summarize briefly

Table 1. Structural and thermodynamic data for ACBP and φ-value mutants thereof.

	WT	V12A	I27A	I74A	V77A	L80A
R_G (Å)[a]	23.6	23.8	24.7	24.6	24.7	26.9
R_H (Å)[b]	25.2	25.6	26.6	26.8	25.1	28.0
$\Delta G_{U/F}$ (kcal/mol)[c]	−8.08	−6.58	n.a.	−6.74	−6.54	−3.51
φ-Value[c]	n.a.	0.59	0.30[d]	0.50	0.28	0.64
ΔG_C α1α4 (kcal/mol)[e]	0.72	1.07	1.22	1.30	1.25	4.08
ΔG_C α2α3 (kcal/mol)[e]	1.00	0.73	1.36	0.88	0.91	1.45
ΔG_C α2α4 (kcal/mol)[e]	0.53	0.51	0.68	0.80	0.68	1.33
ΔG_C 12–27 (α1α2) (kcal/mol)[f]	2.81	1.73	1.75	1.58	1.60	1.49
ΔG_C 12–77 (α1α4) (kcal/mol)[f]	0.66	0.91	1.04	1.20	1.11	2.13
ΔG_C 29–57 (α2α3) (kcal/mol)[f]	0.96	0.73	1.33	0.85	0.88	1.44
ΔG_C 27–80 (α2α4) (kcal/mol)[f]	0.48	0.44	0.53	0.67	0.60	1.58

[a] Calculated from the ASTEROIDS [24] selected ensemble of unfolded ACBP.
[b] Determined from translational diffusion measured by PFG-NMR.
[c] From Kragelund *et al.* [25].
[d] From Fieber *et al.* [16].
[e] Calculated using Eq. (1).
[f] Calculated ΔG_C of specific residue contacts using Eq. (1). The corresponding regions involved are in parentheses.

Please cite this article as: Ozenne Valéry, et al, Exploring the Minimally Frustrated Energy Landscape of Unfolded ACBP, J Mol Biol (2013), http://dx.doi.org/10.1016/j.jmb.2013.10.031

(Fig. 3). The first events in folding involve close proximity of regions corresponding to helices α1 and α4, followed by a transition-state ensemble (TSE) consisting of the interhelical contacts α2α4 [10,25]. Post TSE, poor helix α1 packing distinguishes an intermediate on the native-state side of the folding barrier [31]. These features can be seen in the wild-type computed free-energy landscape and from interhelical contact formation (Fig. 3). The first events in the TSE involve α2α4 contacts, followed by α2α3. Though α1α4 begins to associate early, likely due to the large cluster of contacts between the α1/α2 loop, α1 packs late, α1α4 first followed by α1α2. α1α2 packing is most closely associated with the post TSE barrier.

The contact map of the folding simulation's unfolded ensemble is calculated in the same manner as the ASTEROIDS ensemble maps. The overall features of the contact map generated from the simulation are similar to those generated from the selected ASTEROIDS ensembles. The coarse-grained model gives an overall smaller ensemble R_G of 18 Å as compared to the ASTEROIDS estimate of 23 Å. It is well known that acid- or denaturant-induced ensembles are more expanded compared to the thermal denaturation used in the simulation. Removing all configurations with $R_G < 20$ Å in the denatured simulation ensemble gives a new ensemble average R_G of 23 Å (Fig. 3). This restricted ensemble is more similar to the fitted experimental ensemble, which shows moderate preference for α1α4 and α2α4 in the denatured ensemble.

Conserved hydrophobic residues mediate early long-range contacts

The hydrophobic core of folded ACBP consists, among others, of V12, I27, I74, V77 and L80 (Fig. 1), all of which have relatively high φ-values, which means that they are involved in early, productive contacts along the folding pathway. In order to highlight the involvement of the conserved hydrophobic residues of the core in early-state long-range contacts, we probed some specific native-state contacts in the folding simulations: V12-I27 (α1α2), V12-V77 (α1α4), V12-L80 (α1α4) and I27-L80 (α2α4) (inset of Fig. 3b). Interestingly, the I27-L80 contact is formed early in the folding and the contact formation is linked to the main folding barrier. Subsequent to I27-L80 follow the other contacts, and formation of the transition state has a much lower free-energy barrier. The presence of a second smaller barrier indicates an intermediate state on the native side of the folding barrier. This intermediate state lacks anchoring and packing of α1, and this intermediate state has been experimentally demonstrated by NMR relaxation dispersion [31]. The transition state involves formation of the α2α4 contacts and, more specifically,

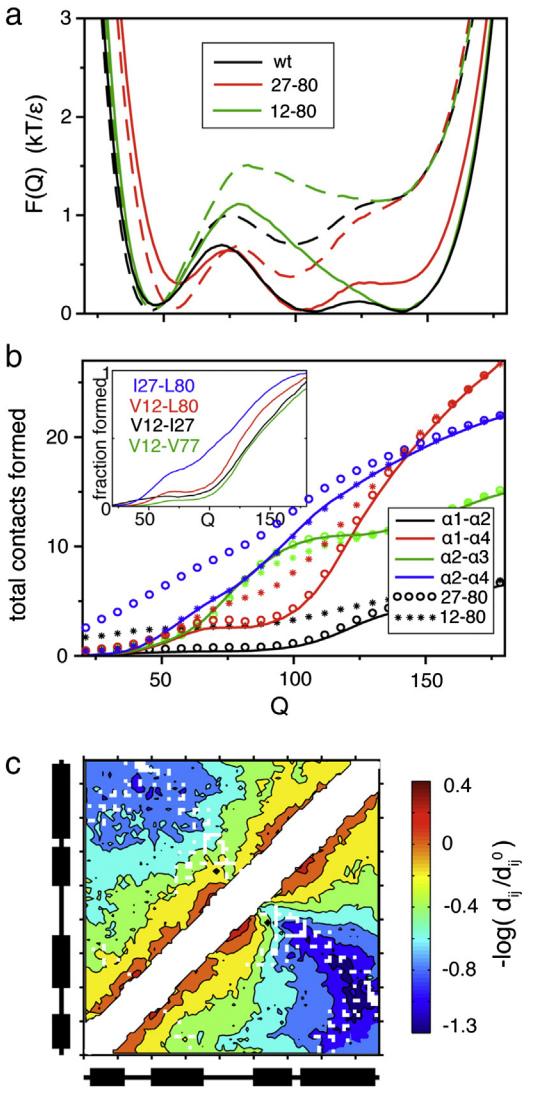

Fig. 3. Structure-based folding simulations of ACBP show unfolding intermediate lacking α1. (a) Folding free energy F for three constructs is shown as a function of the number of native contacts formed Q. Continuous curves show $F(Q)$ at T_m and broken curves show $F(Q)$ where the folded state is thermally destabilized by $\Delta F = k_B T_m$ ($T \sim 1.1 T_m$). Covalent attachment of I27-L80 (α2–α4) stabilizes the intermediate while attaching V12-L80 (α1–α4) turns ACBP into a two-state folder. The intermediate consists of α2-α3-α4 folded and α1 unfolded. (b) Formation of interhelical contacts as a function of the overall folding progress in Q showing that α1 contacts are formed late in the folding process. Dotted line with open circles corresponds to covalent attachment of I27-L80, which makes α2–α4 form earlier. Dotted line with filled stars corresponds to attachment of V12-L80, which makes α1–α2/α4 form earlier. Inset highlights four individual contact formations with Q. (c) Contact map of the denatured state: lower triangle is the entire ensemble at $T = 1.3 T_m$ and upper triangle is a subensemble with all configurations with radius of gyration (R_G) greater than 20 Å. White squares show the native contact map used in the simulation.

Please cite this article as: Ozenne Valéry, et al, Exploring the Minimally Frustrated Energy Landscape of Unfolded ACBP, J Mol Biol (2013), http://dx.doi.org/10.1016/j.jmb.2013.10.031

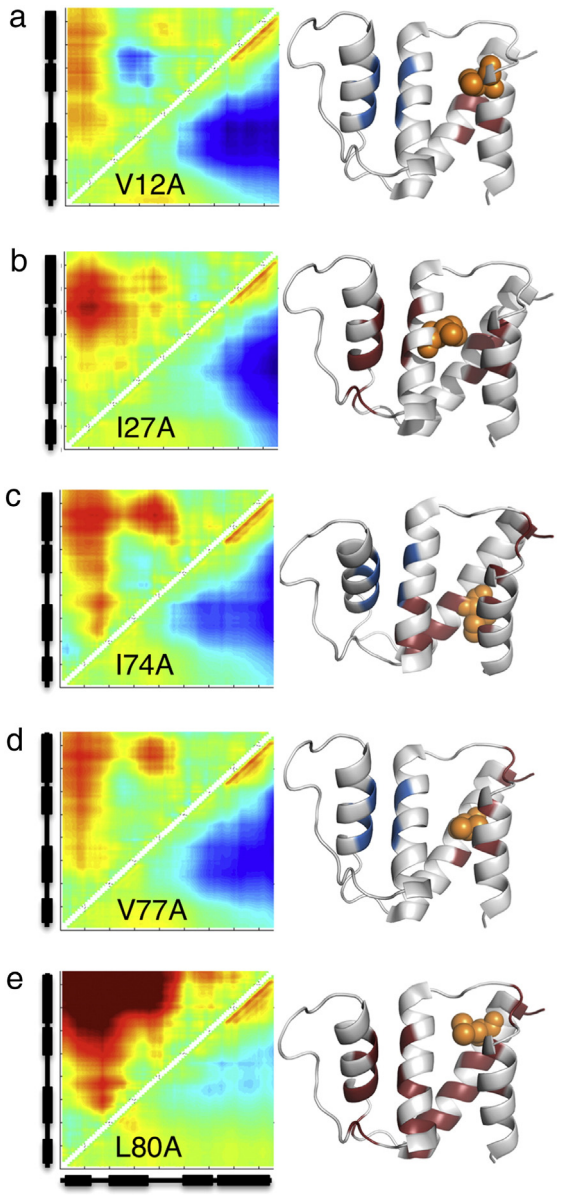

Fig. 4. Contact maps for single-point mutation variants of ACBP. For each contact map, the lower triangle (below the diagonal) shows $\Delta_{ij} = \log(\langle d_{ij}\rangle/\langle d_{ij}^0\rangle)$ where d_{ij} is the determined distance and d_{ij}^0 is the distance for a statistical coil. The upper triangle is the corresponding measure but is compared to wild-type ACBP in order to highlight induced changes in contact formation. In the right panel, for each variant (a)–(e), the mutation is projected onto the structure and significant changes in native contacts are colored on the figure as red, loss of contact, and blue, gain of contact. (a) V12A; (b) I27A; (c) I74A; (d) V77A; (e) L80A.

the I27-L80 contact (Fig. 1). The bias in the contact map of the unfolded ensemble (Fig. 2) agrees well with the early-formed contacts detected in the folding simulations of ACBP.

Mutation of bulky hydrophobic side chains leads to specific loss of native-like long-range contacts

As the long-range contacts in the unfolded ensemble of ACBP seem to be biased toward native-like contacts formed early along the folding pathway, it is an appealing thought that the contacts are strictly controlled to facilitate fast folding and prevent misfolding and/or aggregation. It has been suggested that electrostatic interactions are not involved in early contact formation in protein folding but rather that folding is initiated by a hydrophobic collapse [1,20,32].

Five hydrophobic residues of the core of ACBP were investigated by replacing them one by one with alanine. For each of these mutants, V12A, I27A, I74A, V77A, and L80A, five cysteine variants similar to wild-type ACBP and including S65C were constructed in order to add spin labels following the same protocol as for the wild-type protein. Experimental PREs were measured for each variant (Supplementary Fig. 4) providing a total of 30 × 86 probes, and the data were subsequently used to select structural ensembles of each variant using ASTEROIDS. For each alanine variant, a generalized contact map was calculated.

Perturbation of helix α1 anchoring to the core mainly results in loss of α1α4 contacts

Valine 12 anchors α1 onto the primary α2α4 contact interface (Fig. 1) and is part of the contact surface formed late along the folding pathway. V12 has previously been shown not to be directly involved in any cooperative long-range contacts in the acid-unfolded state [15] and, when replaced with an alanine, yields a φ-value of 0.59 [25]. Figure 4a shows the contact map of the ACBP^{V12A} variant and only small changes are found compared to the wild-type protein. The main effect of this mutation is a loss of α1α4 contacts corresponding to a change in free-energy $\Delta\Delta G_C = 0.35$ kcal/mol and, simultaneously, a gain in α2α3 contacts corresponding to $\Delta\Delta G_C = -0.27$ kcal/mol (Table 1). This suggests that reduction in native-like α1α4 contacts facilitates the native-like α2α3 contacts, underlining the mutually coupled contact events in protein folding.

Perturbation of helix α2 packing to helix α3 results in loss of α2α3 contacts

In the native state, I27 is mainly involved in the packing of α2 to α3 but also in the packing of α2 to α4. The contact map for the ACBP^{I27A} variant is shown in Fig. 4b revealing a significant loss in α2α3 contacts, corresponding to $\Delta\Delta G_C = 0.36$ kcal/mol accompanied by a loss in α1α4 contacts

Please cite this article as: Ozenne Valéry, et al, Exploring the Minimally Frustrated Energy Landscape of Unfolded ACBP, J Mol Biol (2013), http://dx.doi.org/10.1016/j.jmb.2013.10.031

corresponding to $\Delta\Delta G_C$ = 0.5 kcal/mol (Fig. 4 and Table 1). The correlated effects between α2α3 and α1α4 when perturbing helix α1 by V12A or helix α2 by I27A indicate that the α2α3 and α1α4 formations are cooperatively coupled and suggest that α2α3 is a prerequisite for α1α4.

Helix α4-to- α1 packing mutations give small direct effects on α1α4 packing and negatively correlated effects on α2α3 contacts

Both I74 and V77 are involved in the contact interface between helices α4 and α1 (Fig. 1). I74, a non-conserved hydrophobic residue with a φ-value of 0.50, does not pack directly into the primary hydrophobic cluster [25], while V77 packs directly into it (Fig. 1). The effect on the unfolded ensemble by replacing the hydrophobic side chains with alanines is similar for I74 and V77. It mainly affects long-range contacts between α1 and α4 (Fig. 4c and d and Table 1) and, to a smaller degree, formation of α2α4 contacts. The change in free energy is estimated to be $\Delta\Delta G_C$ = 0.5 kcal/mol for α1α4 contacts and 0.2 kcal/mol for α2α4 contacts. Interestingly, we again see a negative correlation between α1α4 and α2α3 contacts. For $ACBP^{I74A}$ and $ACBP^{V77A}$, α2α3 contacts are slightly increased, corresponding to $\Delta\Delta G_C = -0.1$ kcal/mol, in line with the findings for $ACBP^{V12A}$. Thus, the negative correlation between α1α4 and α2α3 is independent of whether the perturbation is in α1α4 or in the α2α3.

Reduction of helix α2 to helix α4 contacts effectively turns the acid-unfolded ACBP into a statistical coil

Long-range contact between helices α2 and α4 appears to be a primary event along the folding pathway (Fig. 3). L80 packs directly toward helix α2 across the hydrophobic core, and this contact is directly involved in the early α2α4 contacts, as displayed by the *in silico* folding calculations. L80A has a φ-value of 0.64, indicating that it is directly involved in a transition-state contact [25]. L80A has a more dramatic effect on the unfolded ensemble as compared to the other variants studied (Fig. 4 and Table 1). Here we see a general loss in long-range contacts and the unfolded ensemble of $ACBP^{L80A}$ displays characteristics of a statistical coil with no specific long-range interactions. The estimated free-energy change for long-range contacts upon L80A mutation is more than 3.3 kcal/mol for α1α4 contacts as compared to 0.35 kcal/mol upon perturbation of helix α1 for $ACBP^{V12A}$. These data underline the interdependence of long-range contacts and provide additional evidence for the simulation result that formation of α2α4 contacts precedes the formation of α1α4 contacts.

Perturbing native-like long-range contacts through mutation of bulky hydrophobic side chains reveals the hierarchical nature of contact formation in ACBP. The initially productive α2α4 contacts mediated by L80 are crucial for the cooperative subsequent long-range α2α3 and α1α4, all of which are the most prominent native-like contacts in the unfolded ensemble.

Reduction in long-range contacts is not directly linked to changes in transient secondary structure

Acid-unfolded ACBP has been shown, by several methods, to have significant residual structure, for example, transient helix formation [7,16]. In particular, this holds not only for the C-terminal α4 region but also for α1, α2, and α3. Mutational perturbations of long-range contacts have been shown to induce chemical shift changes far from the mutation site, and the consistent sign of these chemical shift changes suggests a change in helicity [15]. However, while mutating long-range contacts affects helix formation, we have no direct evidence that changing transient helix formation changes long-range contacts, which has been suggested to be the case for the intrinsically disordered protein ACTR [33]. One method to determine the amount of residual structure is to calculate the SSP from the NMR chemical shifts [34]. Using these C^α shifts, we calculated the SSP for all the studied variants of ACBP (Supplementary Fig. 5) and we found that the V12A, I74A, and V77A substitutions all led to locally increased helicity while the substitutions I27A and L80A locally reduced helicity. This is in line with the predicted helicity using the AGADIR helix propensity prediction tool [35] (Supplementary Fig. 6). This means that both increased and decreased helicity results in reduction of native-like long-range contacts. Perturbations in SSP and long-range contacts induced by the single-point mutations showed no direct link.

Enforcing long-range contacts in the unfolded ensemble has predictable effects on folding

In line with earlier studies, our results show that long-range native interactions exist in the denatured ensemble. While these contacts are only transiently formed, we investigated the effect of permanently constraining them in folding simulations. During the entirety of the simulation, one long-range contact was constrained to be at the native distance, and this was performed for each of the native-like contacts V12-I27 (α1α2), V12-L80 (α1α4), and I27-L80 (α2α4).

Strict enforcement of a late-forming contact (V12-L80) produces a two-state folder, whereas enforcing the early-forming I27-L80 enhances the three-state character of the free-energy landscape

Please cite this article as: Ozenne Valéry, et al, Exploring the Minimally Frustrated Energy Landscape of Unfolded ACBP, J Mol Biol (2013), http://dx.doi.org/10.1016/j.jmb.2013.10.031

(Fig. 3). Forcing helices α1 and α4 together by the V12-L80 contact abolishes the native basin intermediate, and the barrier is increased. Forcing the normal folding nucleus, α2 and α4, together by the I27-L80 contact stabilizes the α1 intermediate. This is in good agreement with, and helps explain, the anti-correlated contact formation found for α1α4 and α2α3 and the general loss of long-range contacts when reducing transition-state formation (α2α4).

Perturbations of determinants of long-range contacts in the unfolded ensemble are reflected in overall hydrodynamic properties of the acid-unfolded ACBP

The contact map of the unfolded ensemble of wild-type ACBP shows that it is more compact than a statistical coil, which is also reflected in the smaller radius of gyration R_G determined both from the generated structural ensembles and from experimentally measured hydration radii R_H. For each of the studied variants of ACBP, the long-range contacts in the unfolded state decrease, which should be reflected in the R_G and consequently also in R_H.

For all studied variants, R_H was determined by experimentally measuring the translational diffusion coefficient, D_t, by PFG-NMR, and R_G was calculated from the generated structural ensembles. R_H falls in between that expected for the wild type and that of a statistical coil (Supplementary Fig. 3 and Table 1) and the experimental R_H and calculated R_G correlate well with a correlation factor of $r^2 = 0.92$, except for one outlier that is omitted in the correlation (Fig. 5). The outlier is ACBP^{V77A} and the mismatch between the measured and calculated R_H may arise from poor PFG-NMR data for that particular sample. The measured and calculated dimensions correlate well with the extent of loss of long-range contacts. For ACBP^{L80A}, R_H is very close to that expected for a statistical coil, in line with the lack of significant long-range contacts in the unfolded ensemble seen in the contact map (Fig. 4e).

The calculated R_G correlates very well with the mutation-induced change in free-energy difference, $\Delta\Delta G_{U/F}$, between the folded and unfolded states displaying the correlation coefficient $r^2 = 0.91$. The correlation of R_G and the folding rate k_f [25] gives $r^2 = 0.82$ (Fig. 5), where k_f is proportional to the first barrier height (#′ in Fig. 6), and correlation between R_G and the mutated residue φ-value gives $r^2 = 0.12$ [25,16] (Supplementary Fig. 7).

The long-range contact preferences in the denatured ensemble could simply reflect a longer average lifetime of stochastically formed native-like long-range contacts or may instead reflect a bias toward contacts present in the TSE. In the latter case, the compactness or the presence of long-range contacts should correlate with the possibility to, from the transiently collapsed unfolded state, fold into the native state, that is, with the native-state stability. The observed anti-correlation between expansion and folding rate is consistent with the long-range contacts found in the acid-denatured ACBP reporting on contacts formed in the TSE, rather than a random subset of native contacts. This is also in line with the earlier discussion that certain native-like contacts show anti-correlated contact preference.

Discussion

Recent studies on ACBP by NMR PRE [12,14], chemical shift analysis [15], FRET [17], and molecular dynamics [18] have revealed the presence of

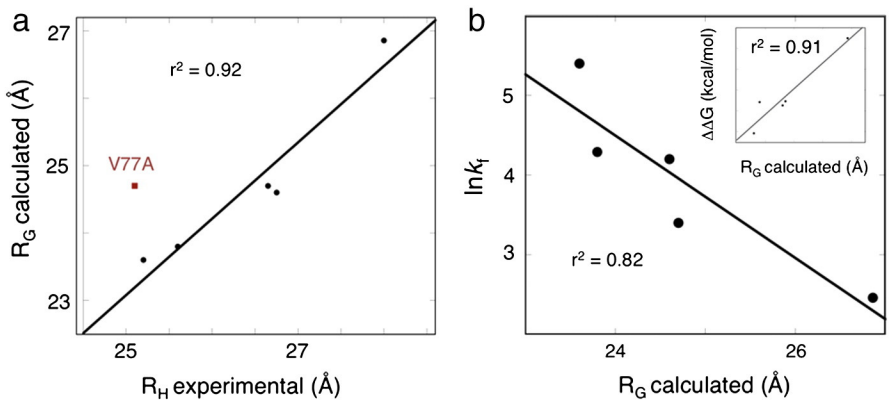

Fig. 5. (a) Correlation plot for the measured hydrodynamic radius and the calculated radius of gyration, R_G, determined from the selected unfolded ensembles. Here the variant V77A did not yield reliable data and was omitted from the correlation and is shown in red in the plot. (b) The correlation of R_G and the folding rate k_f [25] of the protein variant, showing a very strong correlation. Here no data for I27A are available. As an insert in (b), the correlation of R_G and the $\Delta\Delta G$ value is shown.

Please cite this article as: Ozenne Valéry, et al, Exploring the Minimally Frustrated Energy Landscape of Unfolded ACBP, J Mol Biol (2013), http://dx.doi.org/10.1016/j.jmb.2013.10.031

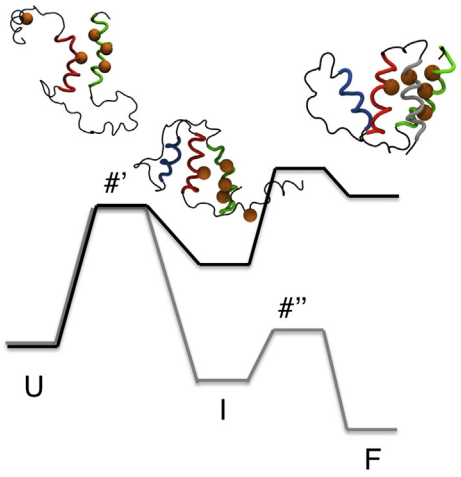

Fig. 6. A schematic model for the ACBP folding pathway. An estimated free-energy profile in water (gray) and that at acid conditions (black) are inserted as a guide to the eye and are not to scale. The transition state (#′), native side folding intermediate, and the native state are shown as insert structures, generated from the folding simulations.

long-range native-like contacts on the unfolded side of the folding barrier. The long-range contacts have been shown to involve mainly helices α2, α3, and α4. In order to further characterize the nature of these long-range contacts, we performed NMR PRE measurements, in combination with single-point mutations, ensemble selections, and *in silico* folding. Although NMR PRE can disturb the system due to the required labeling of the protein, its inherent sensitivity to close range contacts nevertheless makes NMR PRE a good tool to reveal small ensemble changes.

Folding pathway

ACBP is a well-characterized fast-folding protein with both a folding intermediate [36] and an unfolding intermediate [31]. From this combined theoretical and experimental study, we are able to elucidate additional details of the folding pathway for ACBP.

Figure 6 shows a schematic representation of the folding pathway along a putative free-energy profile for the acid-unfolded protein. In several studies, the acid-unfolded ACBP has been shown to harbor significant residual secondary structure [7,15], particularly in the region corresponding to helix α4 [16]. However, the ensembles derived here are selected from a pool of unbiased random-coil structures, which means that the small effects on long-range contacts from local conformational sampling are not explicitly taken into account. Consequently, if we try to validate our ensembles by comparing them with data reporting on local transient conformations, the cross-validation is most likely poor. Even if this validation is not good, it is not a direct measure on the validity of our conclusions, as our ensembles and, in general, the experimental data that have been measured do not carry any direct information on local conformations *per se*.

Our data show that anchoring of α2 to the α4 region is the initial step in folding, in line with previous findings [11,16–18], and this contact is significantly populated also in the acid-unfolded ensemble. Acid denaturation does not seem to promote the compact state as found for Im7 [8], as similar long-range contacts are found in GdmCl [11], a denaturant known to promote extended conformations [37]. Our *in silico* folding results are in line with our experimental results and recent findings [17,14,11] that the α2α4 state corresponds to the transition state. The highly populated α2α4 contacts found in this study are relatively insensitive to mutations outside the α2α4 interface, suggesting that this contact indeed is formed prior to the other native-like contacts found in the unfolded ensemble.

Following the reaction coordinate, the transition state is succeeded by formation of contacts between α2 and α3, corresponding to the participation of helix α3 in the TSE (Fig. 6). These contacts are also present in the unfolded ensemble, but it seems that, prior to α2α3 formation, α2α4 contacts are necessary, since reduction of α2α4 contacts by the L80A mutation effectively reduces α2α3 contacts as well. The set of configurations, where all helices but α1 have formed native-like contacts, may be described as a folding intermediate on the native side of the transition-state barrier (Fig. 6). The presence of this folding intermediate has previously been shown, evidenced by curvature in the denaturant dependence of the unfolding rate constant at low denaturant concentrations as determined by NMR relaxation dispersion [31], as well as in simulations [17]. Furthermore, recent findings show that the native state of ACBP is quite elastic, indicating that α3 packing is loose and of lesser importance for the TSE [38], which is also in line with our data that suggest α2α4 to be the main component of the TSE, and that the intermediate state is residing on the native side of the folding barrier.

Long-range contacts in the unfolded state of ACBP show an interesting anti-correlation between formation of α2α3 and α1α4; that is, reduction of α2α3 formation increases α1α4 contacts and vice versa. This provides direct evidence that the long-range contacts found in the unfolded ensemble of ACBP represent steps in a cooperative process where productive long-range contacts induce native-like compact states. Formation of α2α3 contacts finally induces α1α4 contacts and transition from the folding intermediate to the native state of ACBP (Fig. 6), and this final transition state has previously been assigned, by φ-value analysis, to be a rate-limiting native-like state of ACBP [25].

Please cite this article as: Ozenne Valéry, et al, Exploring the Minimally Frustrated Energy Landscape of Unfolded ACBP, J Mol Biol (2013), http://dx.doi.org/10.1016/j.jmb.2013.10.031

Many long-range contacts found in the unfolded state of ACBP are native-like and on-pathway for folding. Moreover, many conformations detected are interdependent and display properties corresponding to a hierarchical but cooperative order of events initiated by the α2α4 transition state.

The compactness of ACBP is related to the folding rate

The transient long-range contacts formed in the denatured state of ACBP directly affect the level of its compactness, as recently shown also by FRET measurements on ACBP [17]. The tunability and the interdependent nature of the formed contacts indicate the presence of cooperative events also in the denatured state. If the compactness of the denatured ensemble comes from a preference for forming TSE contacts in the denatured ensemble, the level of compactness should correlate with folding rate. Due to the similarity between the acid-unfolded ensemble and the chaotropically unfolded ensemble for wild-type ACBP, we speculate that the similarity also holds for the mutants, and thus, the compactness experiments can be related to the kinetic experiments. If so, the observed correlation among the global parameter R_G, long-range contacts, and folding rate suggests that the biased contact map found for the acid-denatured ACBP does in fact report on a partly collapsed unfolded ensemble biased toward the TSE.

Concluding remarks

A statistical polypeptide coil samples a large number of conformational states where small perturbations would result in significant changes in the free-energy landscape; in other words, the coil is exploring a frustrated landscape [21]. The unfolded state of ACBP, however, is not a true statistical coil, but the primary structure has evolved to minimize the frustration, resulting in a funnel-shaped energy landscape, with the native state in the bottom of the funnel [22]. Our study, along with earlier studies of ACBP, shows that, even in the highly denatured state, ACBP explores a biased region of the conformational space; that is, the energy landscape is significantly less frustrated than expected for a statistical coil. A similar conclusion has been reached for the folding of cytochrome c [39]. Our data show that the long-range contacts found in the unfolded state agree well with the native contacts and that perturbations to native contacts alter the unfolded ensemble and its biased long-range contacts in a predicable way.

Although ACBP has many hallmarks of a two-state folder, recent findings suggest the presence of a short-lived, native-like folding intermediate, I* [31]. Our findings in this study are in line with this and the unfolded ensemble populates contacts corresponding to the folding intermediate. However, the transition-state contacts are even more pronounced, suggesting that the probability for contacts to be formed in the denatured ensemble correlates with the kinetic timing of contact formation along the dominant folding routes. A high contact probability indicates early formation and a low contact probability can indicate late formation. This finding mirrors the interpretation of hydrogen-exchange experiments for the native ensemble, where regions of high exchange (unstable contact) can indicate the first regions to break during unfolding [40]. The NMR PRE contact map reports on both population and proximity in the contacts and thus provides a complimentary tool to map out the folding pathway of ACBP.

In folding studies, using folding kinetic measurements and φ-value analysis, all effects of mutations are assigned to changes in transition-state or native-state energy, generally assuming that the unfolded state is unaffected. Since we show that single-point mutations can alter the unfolded ensemble, these changes may be of importance when interpreting folding kinetic data. However, any mutations to the denatured ensemble that simply expand the ensemble should only have a minimal effect on the stability of the denatured state since the energetic and entropic effects of the mutation tend to cancel, that is, loss of energetically stabilizing contacts *versus* an entropically more stable expanded ensemble.

In conclusion, ACBP presents a clear example of the principle of minimal frustration. Even in the earliest stages of folding, native contacts are either more accessible or more stabilizing on average than non-native contacts. As preferred native contacts are removed, ACBP tends to expand rather than favor other non-native interactions. In the case of ACBP, the molecular basis for the minimal frustration seems surprisingly simple: the ensemble conformational space is directly modulated by a set of conserved hydrophobic residues that form contacts in the native state. These residues direct the folding pathway and, together with the few observed non-native contacts in the unfolded state of ACBP, may serve as gatekeepers [23] protecting from misfolding and aggregation.

Materials and Methods

Protein preparation

Wild type and mutants of bovine ACBP were expressed in *Escherichia coli* strain BL21(DE3)/pLysS, using a pET3a vector with insertion of the wild-type or mutated ACBP gene. Single site mutations were introduced by polymerase chain reaction by use of QuikChange Site-Directed Mutagenesis Kit (Stratagene). Plasmids were sequenced at MWG Biotech. Uniformly ^{15}N labeled protein was expressed at 37 °C in M9 minimal medium containing ^{15}N ammonium sulfate as sole nitrogen source. Purification was performed

Please cite this article as: Ozenne Valéry, et al, Exploring the Minimally Frustrated Energy Landscape of Unfolded ACBP, J Mol Biol (2013), http://dx.doi.org/10.1016/j.jmb.2013.10.031

according to a previous protocol [41]. The purity of fractions and the final protein batch were tested by SDS-PAGE and matrix-assisted laser desorption/ionization time-of-flight mass spectrometry. MTSL spin labels were conjugated to cysteine variants of ACBP by incubating the spin label with the pure protein in room temperature overnight and subsequently separating the conjugated and non-conjugated protein by reversed-phase HPLC.

NMR experiments

Spin-labeling experiments were carried out as described previously [14]. $^{15}N–^{1}H$ heteronuclear single quantum coherence experiments were recorded on a Varian UNITY NMR spectrometer operating at a proton frequency of 800 MHz. Spectra were recorded with the nitroxide in both its oxidized (paramagnetic) and its reduced (diamagnetic) states; the latter was obtained by reduction with a 5-fold molar excess of ascorbate. Assignment and NMR peak intensities were measured as peak height and converted into distance restraints as described previously [14].

^{1}H PGF-LED NMR experiments were performed on wild type and variants of ACBP to determine the hydrodynamic radius (R_H) of the denatured state as described in Ref. [30].

Helix definition and SSP

The helical regions are defined from the folded structure of ACBP (PDB ID: 1NTI). The helical regions used here are defined as α1, residues 3–14; α2, residues 21–36; α3, residues 50–61; and α4, residues 66–84. SSP is calculated from the C^{α} shifts compared to reference random-coil values using the SSP software [34]. The predicted values for helix propensity was calculated using the online prediction tool AGADIR [35].

Ensemble generation

ASTEROIDS ensemble selections were essentially carried out as described previously [24]. A starting pool of 50,000 statistical coil conformers was generated using Flexible-meccano [26,27], and sub-ensembles consisting of 200 conformers were selected using the genetic algorithm ASTEROIDS [42] on the basis of the experimental PRE data. In order to calculate the ensemble-averaged PREs, we have explicitly taken into account the flexibility of the MTSL side chain for each Flexible-meccano conformer [24,43]. The relaxation rates calculated for each conformer were averaged over the entire ensemble and converted into an NMR intensity ratio as described previously [24,14] using an effective mixing time of 10 ms and an intrinsic transverse relaxation rate of the observed proton spin of 12.6 s^{-1}. ASTEROIDS selections were repeated five times and the resulting contact maps were calculated from the distance distribution of the five independent runs.

In silico folding

The *in silico* folding simulations use a standard, coarse-grained, native-biased protein model [44]. The protein is represented by a single bead per residue of radius 4 Å connected by harmonic bonds. Local interactions, angles (i,i + 2) and dihedrals (i,i + 3), are biased to the native values. Tertiary interactions in the native structure are given attractive 10-12 Lennard-Jones interactions. The tertiary interactions are determined from the native structure provided by the Shadow contact map [45]. All non-native interactions are strictly repulsive. The thermodynamics of the protein model was sampled via molecular dynamics using GROMACS 4.5.5 software. The necessary input files are generated from PDB ID: 1NTI using the SMOG Web server 1.2.1‡ [46] and default parameters (same as in Ref. [44]).

The consequence of localizing two pieces of secondary structure, even in the denatured state, was investigated using two mutants, I27-L80 and V12-L80. The specified residues are connected with a harmonic bond, which simulates the effect of a covalent disulfide bond. Therefore, the two residues are strictly maintained at their separation in the native state even when the protein is unfolded.

Acknowledgements

Funding was from SSF (MBD10-0030), the Knut and Alice Wallenberg Foundation (J.D.), and the French Agence Nationale de la Recherche through ANR JCJC ProteinDisorder (to M.R.J.) and ANR MALZ TAUSTRUCT (to M.B.). F.M.P. and B.B.K. were funded from the Carlsberg Foundation. J.K.N. resides at the Center for Theoretical Biological Physics sponsored by the National Science Foundation Grant PHY-1308264 and is also supported by the National Science Foundation Grant MCB-1214457.

Appendix A. Supplementary data

Supplementary data to this article can be found online at http://dx.doi.org/10.1016/j.jmb.2013.10.031.

Received 4 June 2013;
Received in revised form 23 October 2013;
Accepted 24 October 2013
Available online xxxx

Keywords:
protein folding;
residual structure;
transient contacts;
unfolded free-energy landscape;
ensemble selection

† V.O. and J.K.N. contributed equally to this work.
‡ http://smog-server.org

Abbreviations used:
ACBP, acyl co-enzyme binding protein; FRET, fluorescence resonance energy transfer; SSP, secondary structure propensity; PRE, paramagnetic relaxation enhancement; TSE, transition-state ensemble.

References

[1] Ferguson N, Fersht AR. Early events in protein folding. Curr Opin Struct Biol 2003;13:75–81.
[2] Sugase K, Dyson HJ, Wright PE. Mechanism of coupled folding and binding of an intrinsically disordered protein. Nature 2007;447:1021–5.
[3] Lang L, Kurnik M, Danielsson J, Oliveberg M. Fibrillation precursor of superoxide dismutase 1 revealed by gradual tuning of the protein-folding equilibrium. Proc Natl Acad Sci USA 2012;109:17868–73.
[4] Kellis JT, Nyberg K, Sali D, Fersht AR. Contribution of hydrophobic interactions to protein stability. Nature 1988;333:784–6.
[5] Klein-Seetharaman J, Oikawa M, Grimshaw SB, Wirmer J, Duchardt E, Ueda T, et al. Long-range interactions within a nonnative protein. Science 2002;295:1719–22.
[6] Yao J, Chung J, Eliezer D, Wright PE, Dyson HJ. NMR structural and dynamic characterization of the acid-unfolded state of apomyoglobin provides insights into the early events in protein folding. Biochemistry 2001;40:3561–71.
[7] Modig K, Jurgensen VW, Lindorff-Larsen K, Fieber W, Bohr HG, Poulsen FM. Detection of initiation sites in protein folding of the four helix bundle ACBP by chemical shift analysis. FEBS Lett 2007;581:4965–71.
[8] Pashley CL, Morgan GJ, Kalverda AP, Thompson GS, Kleanthous C, Radford SE. Conformational properties of the unfolded state of Im7 in nondenaturing conditions. J Mol Biol 2012;416:300–18.
[9] Maxwell KL, Wildes D, Zarrine-Afsar A, De Los Rios MA, Brown AG, Friel CT, et al. Protein folding: defining a "standard" set of experimental conditions and a preliminary kinetic data set of two-state proteins. Protein Sci 2005;14:602–16.
[10] Kragelund BB, Knudsen J, Poulsen FM. Acyl-coenzyme A binding protein (ACBP). Biochim Biophys Acta 1999;1441:150–61.
[11] Kristjansdottir S, Lindorff-Larsen K, Fieber W, Dobson CM, Vendruscolo M, Poulsen FM. Formation of native and non-native interactions in ensembles of denatured ACBP molecules from paramagnetic relaxation enhancement studies. J Mol Biol 2005;347:1053–62.
[12] Lindorff-Larsen K, Kristjansdottir S, Teilum K, Fieber W, Dobson CM, Poulsen FM, et al. Determination of an ensemble of structures representing the denatured state of the bovine acyl-coenzyme a binding protein. J Am Chem Soc 2004;126:3291–9.
[13] Thomsen JK, Kragelund BB, Teilum K, Knudsen J, Poulsen FM. Transient intermediary states with high and low folding probabilities in the apparent two-state folding equilibrium of ACBP at low pH. J Mol Biol 2002;318:805–14.
[14] Teilum K, Kragelund BB, Poulsen FM. Transient structure formation in unfolded acyl-coenzyme A-binding protein observed by site-directed spin labelling. J Mol Biol 2002;324:349–57.
[15] Bruun SW, Iesmantavicius V, Danielsson J, Poulsen FM. Cooperative formation of native-like tertiary contacts in the ensemble of unfolded states of a four-helix protein. Proc Natl Acad Sci USA 2010;107:13306–11.
[16] Fieber W, Kristjansdottir S, Poulsen FM. Short-range, long-range and transition state interactions in the denatured state of ACBP from residual dipolar couplings. J Mol Biol 2004;339:1191–9.
[17] Voelz VA, Jager M, Yao S, Chen Y, Zhu L, Waldauer SA, et al. Slow unfolded-state structuring in acyl-CoA binding protein folding revealed by simulation and experiment. J Am Chem Soc 2012;134:12565–77.
[18] Lindorff-Larsen K, Trbovic N, Maragakis P, Piana S, Shaw DE. Structure and dynamics of an unfolded protein examined by molecular dynamics simulation. J Am Chem Soc 2012;134:3787–91.
[19] Dunbrack RL. Sequence comparison and protein structure prediction. Curr Opin Struct Biol 2006;16:374–84.
[20] Kurnik M, Hedberg L, Danielsson J, Oliveberg M. Folding without charges. Proc Natl Acad Sci USA 2012;109:5705–10.
[21] Bryngelson JD, Wolynes PG. Spin glasses and the statistical mechanics of protein folding. Proc Natl Acad Sci USA 1987;84:7524–8.
[22] Leopold PE, Montal M, Onuchic JN. Protein folding funnels: a kinetic approach to the sequence–structure relationship. Proc Natl Acad Sci USA 1992;89:8721–5.
[23] Otzen DE, Oliveberg M. Salt-induced detour through compact regions of the protein folding landscape. Proc Natl Acad Sci USA 1999;96:11746–51.
[24] Salmon L, Nodet G, Ozenne V, Yin G, Jensen MR, Zweckstetter M, et al. NMR characterization of long-range order in intrinsically disordered proteins. J Am Chem Soc 2010;132:8407–18.
[25] Kragelund BB, Osmark P, Neergaard TB, Schiodt J, Kristiansen K, Knudsen J, et al. The formation of a native-like structure containing eight conserved hydrophobic residues is rate limiting in two-state protein folding of ACBP. Nat Struct Biol 1999;6:594–601.
[26] Bernado P, Blanchard L, Timmins P, Marion D, Ruigrok RW, Blackledge M. A structural model for unfolded proteins from residual dipolar couplings and small-angle X-ray scattering. Proc Natl Acad Sci USA 2005;102:17002–7.
[27] Ozenne V, Bauer F, Salmon L, Huang JR, Jensen MR, Segard S, et al. Flexible-meccano: a tool for the generation of explicit ensemble descriptions of intrinsically disordered proteins and their associated experimental observables. Bioinformatics 2012;28:1463–70.
[28] Bibow S, Ozenne V, Biernat J, Blackledge M, Mandelkow E, Zweckstetter M. Structural impact of proline-directed pseudophosphorylation at AT8, AT100, and PHF1 epitopes on 441-residue tau. J Am Chem Soc 2011;133:15842–5.
[29] Fieber W, Kragelund BB, Meldal M, Poulsen FM. Reversible dimerization of acid-denatured ACBP controlled by helix A4. Biochemistry 2005;44:1375–84.
[30] Danielsson J, Jarvet J, Damberg P, Graslund A. Translational diffusion measured by PFG-NMR on full length and fragments of the Alzheimer A beta(1-40) peptide. Determination of hydrodynamic radii of random coil peptides of varying length. Magn Reson Chem 2002;40:S89–97.
[31] Teilum K, Poulsen FM, Akke M. The inverted chevron plot measured by NMR relaxation reveals a native-like unfolding intermediate in acyl-CoA binding protein. Proc Natl Acad Sci USA 2006;103:6877–82.

Please cite this article as: Ozenne Valéry, et al, Exploring the Minimally Frustrated Energy Landscape of Unfolded ACBP, J Mol Biol (2013), http://dx.doi.org/10.1016/j.jmb.2013.10.031

[32] Dasgupta A, Udgaonkar JB. Evidence for initial non-specific polypeptide chain collapse during the refolding of the SH3 domain of PI3 kinase. J Mol Biol 2010;403:430–45.
[33] Iesmantavicius V, Jensen MR, Ozenne V, Blackledge M, Poulsen FM, Kjaergaard M. Modulation of the intrinsic helix propensity of an intrinsically disordered protein reveals long-range helix–helix interactions. J Am Chem Soc 2013;135:10155–63.
[34] Marsh JA, Singh VK, Jia Z, Forman-Kay JD. Sensitivity of secondary structure propensities to sequence differences between alpha- and gamma-synuclein: implications for fibrillation. Protein Sci 2006;15:2795–804.
[35] Munoz V, Serrano L. Development of the multiple sequence approximation within the AGADIR model of alpha-helix formation: comparison with Zimm-Bragg and Lifson-Roig formalisms. Biopolymers 1997;41:495–509.
[36] Teilum K, Maki K, Kragelund BB, Poulsen FM, Roder H. Early kinetic intermediate in the folding of acyl-CoA binding protein detected by fluorescence labeling and ultrarapid mixing. Proc Natl Acad Sci USA 2002;99:9807–12.
[37] Wilkins DK, Grimshaw SB, Receveur V, Dobson CM, Jones JA, Smith LJ. Hydrodynamic radii of native and denatured proteins measured by pulse field gradient NMR techniques. Biochemistry 1999;38:16424–31.
[38] Heidarsson PO, Valpapuram I, Camilloni C, Imparato A, Tiana G, Poulsen FM, et al. A highly compliant protein native state with a spontaneous-like mechanical unfolding pathway. J Am Chem Soc 2012;134:17068–75.
[39] Weinkam P, Zimmermann J, Floyd ER, Wolynes PG. The folding energy landscape and free energy excitations of cytochrome C. Acc Chem Res 2010;43:652–60.
[40] Kragelund BB, Knudsen J, Poulsen FM. Local perturbations by ligand binding of hydrogen deuterium exchange kinetics in a four-helix bundle protein, acyl coenzyme A binding protein (ACBP). J Mol Biol 1995;250:695–706.
[41] Mandrup S, Hojrup P, Kristiansen K, Knudsen J. Gene synthesis, expression in *Escherichia coli*, purification and characterization of the recombinant bovine acyl-CoA-binding protein. Biochem J 1991;276:817–23.
[42] Nodet G, Salmon L, Ozenne V, Meier S, Jensen MR, Blackledge M. Quantitative description of backbone conformational sampling of unfolded proteins at amino acid resolution from NMR residual dipolar couplings. J Am Chem Soc 2009;131:17908–18.
[43] Iwahara J, Schwieters CD, Clore GM. Ensemble approach for NMR structure refinement against (1)H paramagnetic relaxation enhancement data arising from a flexible paramagnetic group attached to a macromolecule. J Am Chem Soc 2004;126:5879–96.
[44] Clementi C, Nymeyer H, Onuchic JN. Topological and energetic factors: what determines the structural details of the transition state ensemble and “en-route” intermediates for protein folding? An investigation for small globular proteins. J Mol Biol 2000;298:937–53.
[45] Noel JK, Whitford PC, Onuchic JN. The shadow map: a general contact definition for capturing the dynamics of biomolecular folding and function. J Phys Chem B 2012;116:8692–702.
[46] Noel JK, Whitford PC, Sanbonmatsu KY, Onuchic JN. SMOG@ctbp: simplified deployment of structure-based models in GROMACS. Nucleic Acids Res 2010;38:W657–61.

Please cite this article as: Ozenne Valéry, et al, Exploring the Minimally Frustrated Energy Landscape of Unfolded ACBP, J Mol Biol (2013), http://dx.doi.org/10.1016/j.jmb.2013.10.031